proton that deposited the proper amount of energy in the recoil detector(s), but for which the relative timing of the protons differed from "true" coincidences by one beam burst. FPP spin-sorted left-right spectra for both "reals" and "accidentals" were made for all three sections of the Si detector. This allowed us to optimize subtraction of accidentals, since at most angles a large majority of the recoil protons were incident on the center section, which consisted of a single strip.

There are several systematic error checks available to us in the data. The ^{12}C elastic peak was present on the focal plane from 5° to 19°, and for both the ^{12}C elastic peak and the p+p peak, the induced polarization, P, and the analyzing power, A_y, were measured. These two observables should be equal; and since they are sensitive to different possible sources of systematic error, their comparison is an important means of systematic error evaluation. We also simultaneously measured $D_{NN'}$ for ^{12}C elastic scattering, which must be exactly 1. Careful evaluation of other possible systematic errors is presently underway.

Preliminary results of our analysis up to this point are presented in Fig. 2.

1. J.R. Bergervoet, P.C. van Campen, R.A. Klomp, J.L. de Kok, T.A. Rijken, V.G.J. Stoks, and J.J. de Swart, Phys. Rev. C **41**, 1435 (1990).
2. R.A. Arndt, Z. Li, L.D. Roper and R.L. Workman, Phys. Rev. Lett. **65**, 157 (1990).
3. R. Machleidt and F. Sammarruca, Phys. Rev. Lett. **66**, 564 (1991).
4. L. Wolfenstein, Ann. Rev. of Nucl. Sci. **6**, 43 (1956).
5. D.V. Bugg, *et al.*, J. Phys. **G4**, 1025 (1978).
6. Kazuo Gotow, Frederick Lobkowicz, and Ernst Heer, Phys. Rev. **127**, 2206 (1962).
7. Y. Onel, R. Hausammann, E. Heer, R. Hess, C. Lechanoine-Leluc, W.R. Leo, and D. Rapin, Phys. Rev. D **40**, 35 (1988).
8. G.P.A. Berg, *et al.*, IUCF Sci. and Tech. Rep., May 1992–April 1993.

SPIN CORRELATION COEFFICIENTS IN $\bar{p}\vec{p}$ ELASTIC SCATTERING AT 200 MeV

W.A. Dezarn, J. Doskow, J.G. Hardie, H.O. Meyer, R.E. Pollock,
B. von Przewoski, T. Rinckel, and F. Sperisen
*Indiana University and Indiana University Cylotron Facility,
Bloomington, Indiana 47408*

W. Haeberli, B. Lorentz, F. Rathmann, M.A. Ross, and T. Wise
University of Wisconsin-Madison, Madison, Wisconsin 53706

P.V. Pancella
Western Michigan University, Kalamazoo, Michigan 49008

An experiment to measure spin correlation coefficients in $\vec{p}\vec{p}$ elastic scattering with a stored, polarized beam on an internal, polarized target has been mounted in the A-region

of the IUCF Cooler. The measurement is carried out at 200 MeV bombarding energy. In this energy range data for spin correlation coefficients, which are essential for constraining the spin dependent terms of the nucleon-nucleon interaction, are quite sparse. Since the installation of the University of Wisconsin Atomic Beam Source (ABS) in June 1993, the experimental equipment has been commissioned in five running periods. Some of the technical problems that were overcome are presented in this report. The experiment is now on the verge of producing final data.

A description of the experimental design was presented earlier.[1] The basic components are the following. The ABS supplies a flow of polarized atomic hydrogen into a 25.4-cm long target cell with a cross section of 8 mm × 8 mm. The target cell has thin walls of teflon to transmit low-energy recoil protons while containing the atomic hydrogen and maintaining its polarization.[2] The Cooler beam passes through the open length of the target cell and interacts with the polarized atoms. A guide field to define the target polarization is provided by magnet coils mounted on the exterior of the scattering chamber. Forward scattered protons are detected in a cylindrically symmetric detector consisting of four wire chamber planes and an array of scintillators. This detector arrangement was previously used by the CE-01 experiment.[3] Silicon microstrip detectors are placed outside the target cell, 5 cm from the beam, to detect the recoil protons. The requirement of a coincidence between the CE-01 detector and the silicon detectors provides for clean identification of scattering events. Four scintillator detectors are placed just outside a thin-walled nose cone attachment to the scattering chamber at an angle of 45° relative to the center of the cell. They are used as independent monitors of the target thickness and of beam and target polarization when both are polarized.

The guide field is provided by three sets of Helmholtz coils mounted on the outside of the scattering chamber around the target cell location (see Fig. 1). These coils generate magnetic fields of uniform direction (but non-uniform magnitude) which define the three target spin directions : X (sideways), Y (vertical), and Z (longitudinal). For both transverse field directions, a second set of compensating coils is mounted just upstream of the first to minimize a field-dependent shift of the beam at the target. The remaining beam shift is proportional to the strength of the guide field. In order to determine the lowest acceptable field, the target polarization was measured as a function of the current in the X coils. Figure 2 shows the X and Y components of the target polarization. The respective target polarizations were deduced from measured asymmetries in pp elastic scattering (see below). It is important to note that the target polarization in the Y direction is small, but nonzero. This is now understood to be caused by a small ambient field of about 0.5 Gauss. An effort is being made to compensate for this field.

The cyclic data-taking process was organized as follows. Polarized beam of either up or down polarization state was stack-injected into the Cooler with beam currents as high as 200 μA. Data were taken for 500 seconds, and then the stored beam was dumped. The beam spin was reversed for every new cycle. During data acquisition, the guide fields were changed as follows : $B_x(+)$, $B_x(-)$, $B_y(-)$, $B_y(+)$, $B_z(+)$, $B_z(-)$, where the subscript refers to the field direction and the plus or minus sign tells the field sign. Each magnetic field state was maintained for 2 seconds and the entire pattern was repeated 41 times. The remaining 8 s in a 500 s cycle were used to turn on and off detectors, dump the stored
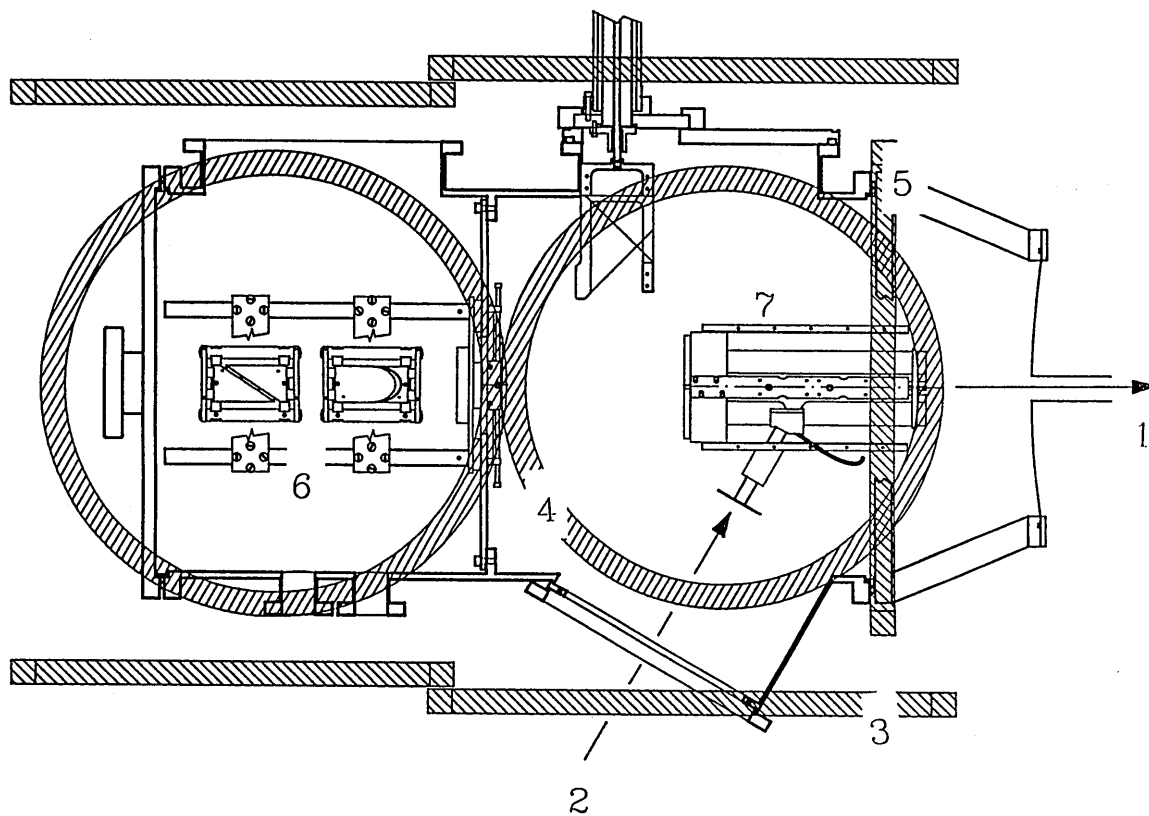
Figure 1. Drawing of scattering chamber. Labels are as follows: (1) Cooler beam, (2) ABS beam, (3) X coil, (4) Y coil, (5) Z coil, (6) Beam position monitors, and (7) Target cell.
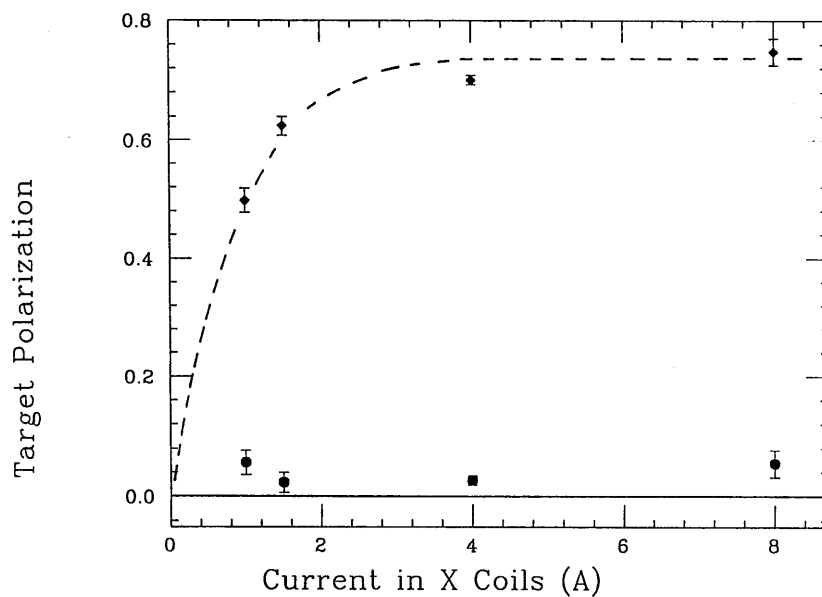

Figure 2. Target polarization as a function of current in X coils. (o) is the vertical target polarization and ($\diamond$) is the horizontal target polarization. The curves are to guide the eye.

beam and measure the PCT offset (see below). During Cooler injection, the target was turned off.

The event trigger was defined by a coincidence between a signal in one of the 8 silicon detectors and the opposite quadrant of the CE-01 detector. For example, a signal from one of the two silicon detectors with azimuthal angle $\phi = -135°$ and a region in the CE-01 detector in the range $25° \leq \phi \leq 65°$ satisfies this trigger. The performance of the silicon microstrip detectors is described elsewhere in this report. A plot of the scattering angle of the forward-scattered proton as a function of the recoil proton energy in the silicon detector characterizes pp events of interest. As an example, Fig. 3 shows the two kinematic loci obtained during a run where both hydrogen and helium targets were present during data acquisition.

After the polarization direction of the target is changed, it takes a certain time before the new equilibrium is reached. An analysis of the horizontal target polarization as a function of time after a guide field flip is shown in Fig. 4. From these data we see that it takes less than 50 ms for the target polarization to equilibrate completely with the new field. Waiting 100 ms after the field change ensures that full polarization is reached. A "target-spin-valid" flag is used to block out data acquisition during the state change.

The goal of CE-35 is to measure the spin correlation coefficients A_{xx}, A_{yy}, and A_{xz} of $\bar{p}p$ elastic scattering at 200 MeV. The method for extracting these observables from the data is as follows. First, the raw yields from the detectors for each beam and target spin state are extracted from XSYS. Then, correction factors for relative beam current, relative target thickness and relative detector efficiency are approximately determined from sums over detectors and spin states. Corrected yields are obtained by dividing by these factors. Thus, when summing over all spin states, each detector has the same yield, and when summing over detectors each opposite-sign spin state has the same yield. Simple sums and ratios of the corrected yields then yield the observables, the beam polarization and two of the three target polarizations. In order to fix the absolute scale, a value for the analyzing power, A_y, must be assumed. In a previous IUCF experiment,[4] A_y has been measured very accurately at one angle and energy. Taking this as the calibration point, a phase shift analysis was used to extrapolate A_y in energy and scattering angle. Three phase shift analyses (Bonn, Nijmegen, and an energy-dependent solution from the SAID database called C200[5]) were scaled to match the calibration point. All three solutions matched the analyzing power data from CE-08[6] equally well. Thus, we conclude that the result of the present experiment does not depend on the choice of phase shift analysis used to extrapolate the calibration point. Arbitrarily, the C200 solution from SAID was chosen mainly because it is recorded with an error estimate. The Z target polarization can be directly measured only after beam with longitudinal polarization becomes available. At present it must be inferred from a careful measurement of the guide field. Figure 5 shows the assumed A_y together with the results from this experiment. Even though the latter is normalized to the former, it could still, in principle, differ in shape. At present we consider our results for the spin correlation coefficients to be preliminary.

To check for systematic asymmetries in the experimental setup, data were also taken with an unpolarized target. To obtain unpolarized target atoms, a beam stop was inserted in the ABS axis and H_2 or ^4He gas was allowed to flow into the target cell through a teflon
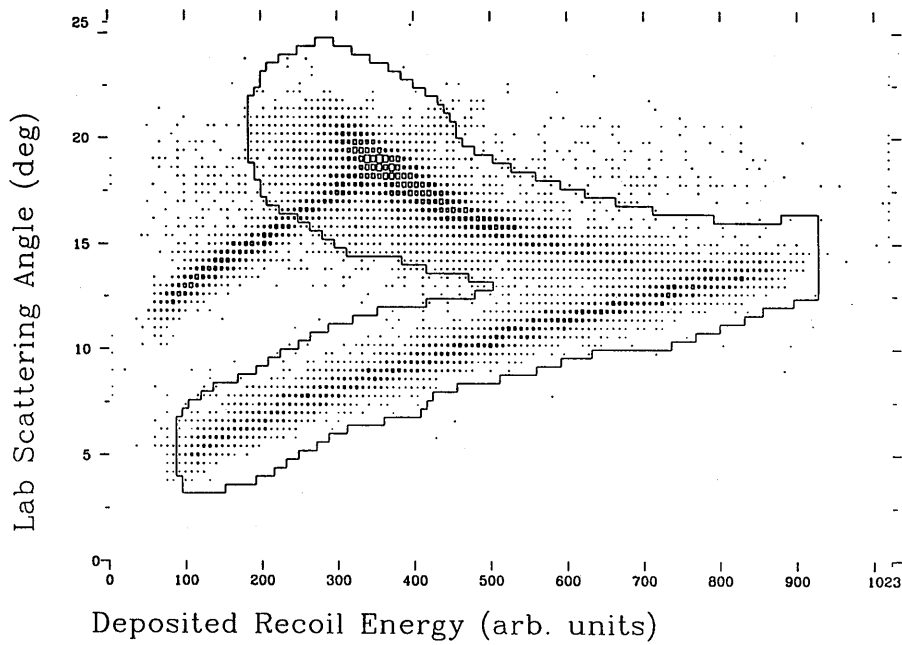
Figure 3. Lab scattering angle (θ) versus deposited recoil energy E_R. Locus in polygon is due to pp events. Branch across pp locus is due to p + ^{4}He events.
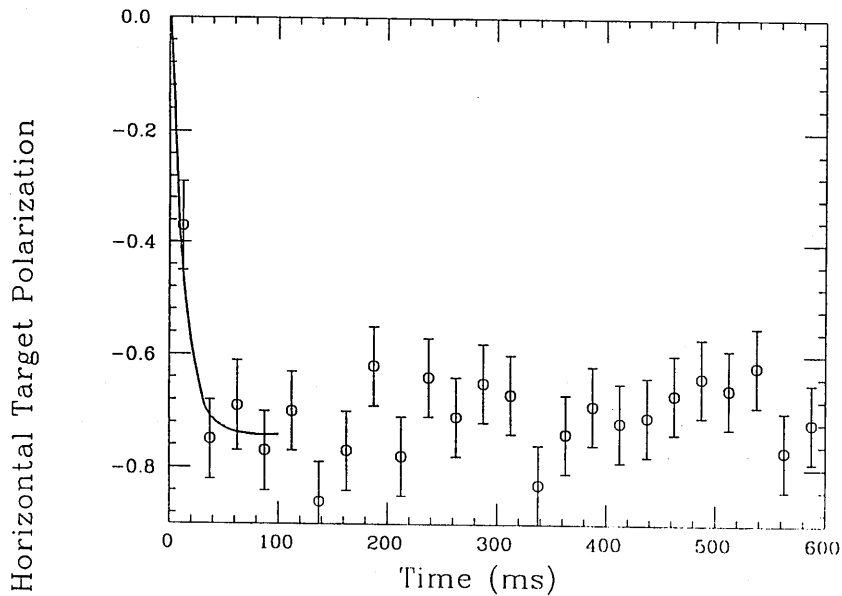

Figure 4. Horizontal target polarization as a function of time after a field sign flip. The curve is to guide the eye.
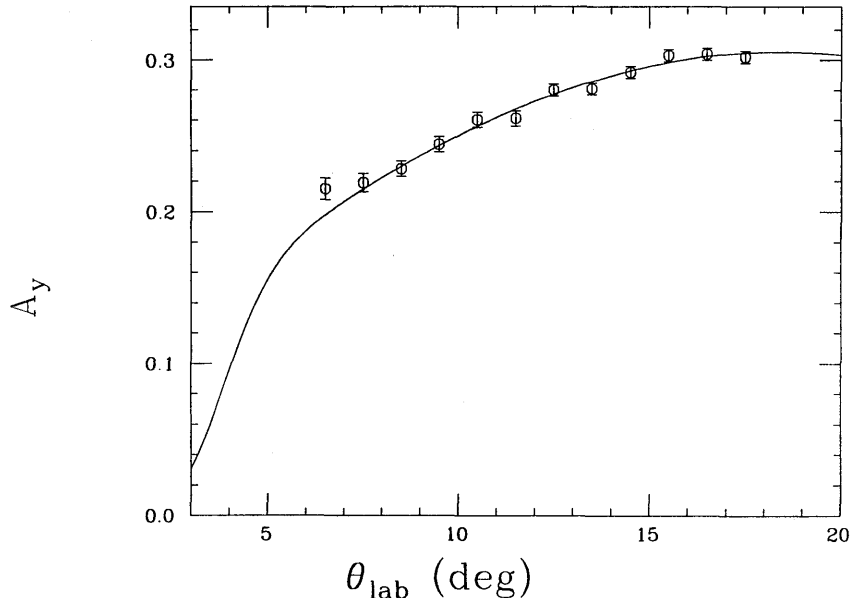
10

Figure 5. Analyzing power A_y as a function of scattering angle (θ). Solid line is assumed from the scaled C200 solution. Data points are from reanalyzing data for A_y after determining polarization values to check experimental values against the original assumption.

tube connected to the feed tube of the cell gas. The same data-taking cycle was used for this test and data were analyzed with the same code and conditions as for a polarized target. From this analysis we measured the X target polarization to be -0.0098 ± 0.0068 and the Y target polarization to be 0.0073 ± 0.0068. Within this level of statistics no intrinsic experimental asymmetry is observed.

The presence of the guide fields also has an undesirable effect on the experiment. As mentioned earlier, the X and Y guide fields affect the closed orbit of the Cooler beam. Compensation coils were added to reduce the beam shift, but such an arrangement is not completely local and guide-field-dependent beam shifts were measured everywhere in the Cooler. In the A-region, for instance, a current oscillating between $\pm$ 8 A in the X coils resulted in a beam shift of $\pm$ 0.1 mm in the vertical direction. The worry is that when the beam shifts, there could be a change in the possible admixture of unwanted events that still pass the acceptance criterion for scattering. To study the effect of a beam shift on the experiment, combinations of steering that give a local shift at the cell location were operated at their maximum positive and negative values, corresponding to measured beam shifts of 2.2 mm horizontally and 3.5 mm vertically; i.e., much larger than the beam shifts due to the guide fields. Data taken with these artificial beam shifts revealed no change within statistics. Thus, effects due to beam shifts are below our present level of accuracy.

Another unwanted effect of the guide fields is that the X field interferes with the operation of the medium field magnet (MF) in the ABS. The purpose of the MF is to remove one of the two atomic hydrogen hyperfine spin states that remain after the sextupole separation, so that only one spin state goes into the target cell.[7,8] If the MF is not at the proper field setting (e.g. by a contribution from the X field), the MF will not properly separate the two atomic spin states. This leads to a reduction in target polarization and

an increase in target thickness. Magnetic field maps along the ABS axis have shown a MF field change when the X coils are operated and no effect when the Y or Z coils are operated.

A possible beam shift, as well as the effect on the MF field, make a small guide field desirable. However, if the guide fields are operated too low, the small constant field measured near the target chamber can no longer be ignored and will create unwanted polarization components. In the future, we will make an attempt to compensate the ambient field.

The Parametric Currrent Transformer (PCT) was used to measure the beam current in the Cooler. For the purpose of processing, the PCT DC signal is converted to a frequency. A typical example of beam current versus cycle time is given in Fig. 6 where we have plotted counts in the PCT versus time. The pulses that are superimposed on the exponential decay of the beam current are due to a 20 μA calibration current applied to the PCT to allow determination of the absolute beam current. The resulting calibration constant is 49.7 $\pm$ 1.1 counts/μC. This agrees well with the value measured by CE-25.[9] One important feature of the PCT is a DC offset that is difficult to control, since it depends sensitively on temperature. This offset is measured by dumping the Cooler beam at the end of each cycle and then continuing to take data for 3 seconds thereafter.

The target thickness can be deduced from the measured beam current, the scattering rate in the 45° detectors, the geometrical acceptance calculated with a Monte Carlo simulation, and the known cross section. This was used to monitor the long-term performance of the ABS. Fig. 7 shows the target thickness as a function of time elapsed after the start of the CE35 run in April, 1994. It can be seen that for the first 48 hours the target thickness is fairly constant at a value of 3×10^{13} atoms cm^{-2}, as was expected.[10] After that, the target thickness slowly decreases, presumably due to the buildup of frozen water in the nozzle of the dissociator, which is operated at liquid nitrogen temperature. Warming up the nozzle restored the original performance as seen in Fig. 7.

Internal polarized buffer cell targets imply a small aperture. This restricts the Cooler acceptance and makes the operation more difficult. We are still gaining experience in optimizing the Cooler operating parameters. At present we observe accumulation rates ranging from 20 μA/min to 40 μA/min and beam lifetimes between 500 s and 3000 s. So far, an external alignment fixture has been used to align the target cell such that its axis coincides with the optical reference axis of the Cooler. However, there are now indications that the preferred beam position is different from the reference axis. In response to this, the cell was raised by 3 mm and steps were taken to make the bending magnets stronger that allow vertical adjustment of the beam at the target. This is expected to increase the Cooler acceptance. In order to protect the silicon detectors in the A-region from beam that enters the ring during injection but is not kicked into orbit, a blocking device is mounted in the T-region.

Since commissioning started, two new elements have been added to the detector setup in the A-region. The first is a 7.5-cm thick aluminum absorber placed between the wire chambers and the E-detector of the CE-01 array. Its purpose is to degrade the scattered protons enough to be stopped in the E-detector. This improves the rejection of background events. Second, a 10.2 cm $\times$ 10.2 cm $\times$ 0.3 cm scintillator has been placed after the wire
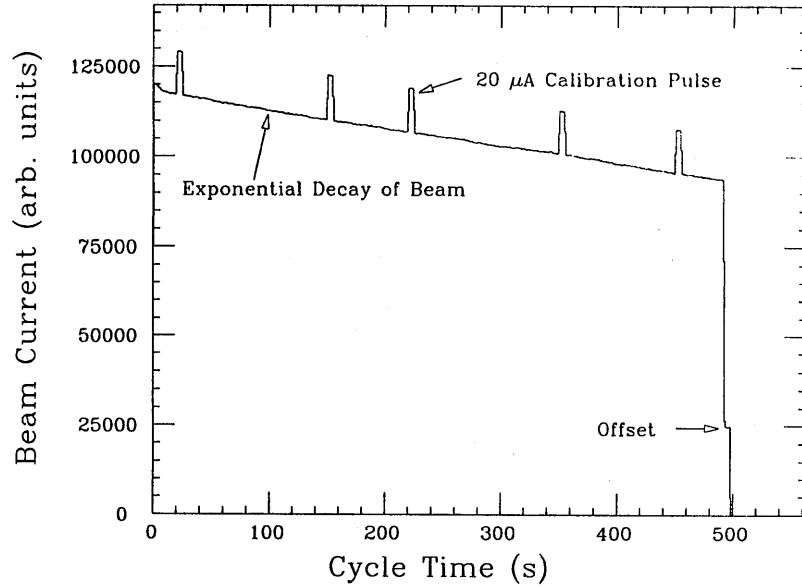
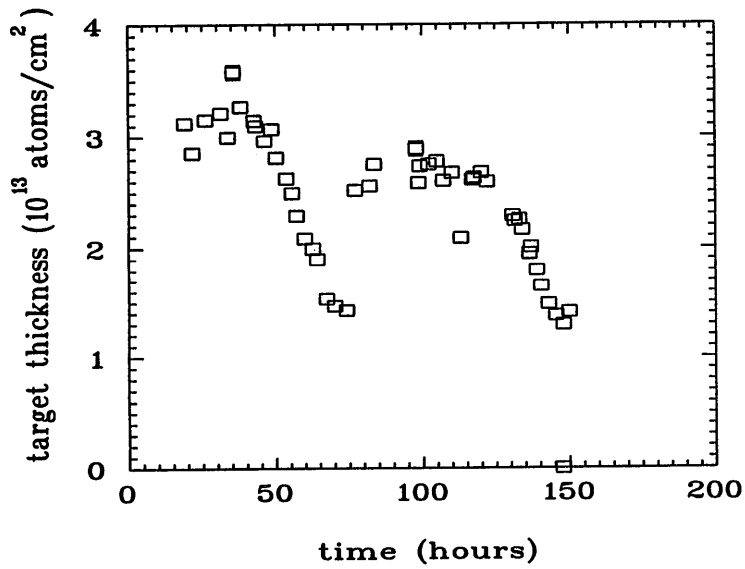*Figure 6.* Beam current as a function of cycle time from the PCT.

Figure 7. Target thickness as a function of time of ABS operation during April 1994. Periods of constant target thickness are 48 hours. Second plateau in target thickness occurred after warming ABS dissociator nozzle to unclog it.

chambers and before the aluminum absorber in such a way that it intercepts the acceptance cone at large angles. Comparing the scattering angle determined by the wire chambers for events that fire this detector with the known detector position leads to a check of the correctness of the wire-chamber tracking algorithm.

1. M.A. Ross, *et al.*, IUCF Sci. and Tech. Rep., May 1992 – April 1993, p. 161.
2. M.A. Ross, *et al.*, IUCF Sci. and Tech. Rep., May 1992 – April 1993, p. 157.
3. H.O. Meyer, *et al.*, Nucl. Phys. **A539**, 633 (1992).
4. B. v. Przewoski, *et al.*, Phys. Rev. C **44**, 44 (1991).
5. R.A. Arndt, *et al.*, Phys. Rev. D **45**, 3995 (1992), and the SAID database mentioned therein.
6. W.K. Pitts, *et al.*, Phys. Rev. C **45**, R1 (1992).
7. A.D. Roberts, *et al.*, Nucl. Instrum. & Methods **A322**, 6 (1992).
8. T. Wise, *et al.*, Nucl. Instrum. & Methods **A336**, 410 (1993).
9. G. Savopulos, CE-25 PCT analysis, private communication.
10. M.A. Ross, *et al.*, Nucl. Instrum. & Methods **A344**, 307 (1994).